How the Decays of Heavy Right-Handed Neutrinos Lead to Leptogenesis

Ana Sofia Carvalho-Soares

Received November 18, 2024
Accepted March 11, 2025
Electronic access March 31, 2025

Leptogenesis is a theoretical framework that explains the observed matter-antimatter asymmetry in the universe through the decay of heavy right-handed neutrinos. This mechanism not only addresses the origin of the matter-dominated universe but also offers an intuitive explanation for the smallness of neutrino masses and the absence of right-handed neutrinos at low energy scales. Here we discuss a plausible extension to the Standard Model, the type I seesaw mechanism, and its connection to leptogenesis. We discuss key concepts related to matter-antimatter asymmetry, including baryon asymmetry and CP violation – the violation of charge-parity symmetry. We also overview recent experimental searches, emphasising neutrinoless double beta decay experiments and the limitations they impose on the theory.

Introduction

Leptogenesis proposes that the decay of heavy right-handed neutrinos in the early universe generated a surplus of leptons over anti-leptons. This lepton asymmetry was subsequently converted into a baryon asymmetry, ultimately leading to the matter-dominated universe we observe today [1]. The study of leptogenesis not only seeks to explain the origin of this asymmetry but also bridges a gap between particle physics and cosmology.

The impetus for studying leptogenesis arises from significant advancements in neutrino physics, most notably the discovery of neutrino oscillations [2], which confirmed that neutrinos are massive particles. This discovery challenged the Standard Model of particle physics, indicating that new physics beyond the Standard Model is required to fully understand particle interactions. Leptogenesis extends this understanding by proposing a mechanism that not only accounts for neutrino masses but also provides a natural explanation for the observed matter-antimatter asymmetry in the universe. The theoretical foundation of leptogenesis considered here rests on a proposed extension to the Standard Model called the seesaw mechanism [3,4], which predicts a heavy right-handed neutrino that participates in lepton number violating decays in the early universe. Leptogenesis has significant implications for the Standard Model, suggesting the existence of new particles and interactions that go beyond the current theoretical framework. Exploring leptogenesis could thus offer insights into new physics and guide experimental searches for phenomena beyond those presently accessible. We provide a comprehensive overview of leptogenesis, highlighting its role in explaining the matter-antimatter asymmetry of the universe and examining the experimental evidence supporting the model.

Methodology

A systematic approach was employed to identify relevant literature on the various topics covered. Searches were conducted in academic databases, including Google Scholar and arXiv, using a combination of keywords related to each topic. Preference was given to peer-reviewed publications, highly cited studies, and works authored by well-established researchers or institutions. Additional sources were identified through citation tracking and references from key papers.

Studies were selected based on their relevance to each topic. The selection prioritized the most up-to-date results and studies that presented theoretical developments, experimental validations, or comprehensive reviews of existing models. This ensured that the discussion was grounded in current scientific understanding.

For each selected study, relevant information was extracted and organized in a structured format to facilitate synthesis. Key details, including theoretical frameworks, experimental findings, and implications for the broader field, were documented to provide a clear and coherent analysis.

The synthesis method employed in this review follows a narrative synthesis approach, structuring the discussion thematically rather than comparing individual studies. The literature was organized into three main topics: neutrino physics and its open questions, matter-antimatter asymmetry and its unresolved issues, and finally, leptogenesis as a potential solution connecting both problems. Following this, experimental evidence that could support leptogenesis was discussed. This approach ensured a logical progression from fundamental principles to the proposed solution, providing a structured and comprehensive summary of the relevant concepts.

Neutrino Physics

Neutrinos were initially predicted by Wolfgang Pauli in 1930 to explain the apparent loss of energy and momentum in beta decay. He proposed this new particle in a letter to the Physical Institute of the Federal Institute of Technology, Zürich[5], but it was only in 1934 that the particle was formally introduced in the scientific literature by Enrico Fermi[6]. Finally, it was experimentally detected in 1956[7], confirming Pauli's hypothesis and disproving his belief that such particles were undetectable.

The Standard Model of particle physics (SM) assigns neutrinos zero mass, which was consistent with experimental evidence for a long time - they were observed to travel near the speed of light, interact only weakly, and pass through ordinary matter almost unimpeded. However, in 1998, experimental evidence from the Super-Kamiokande experiment indicated that neutrinos do have mass[2], a discovery with profound implications for both particle physics and cosmology, necessitating extensions of the Standard Model. There are still several unresolved problems in the modern theory of neutrinos, including the exact nature of their mass, their role in the matter-antimatter asymmetry of the universe, and the possible existence of sterile neutrinos. Simultaneously, neutrinos serve as unique probes for exploring the interiors of stars, supernovae, particle physics, and the early universe.

Neutrinos General Overview

Neutrinos are spin $\frac{1}{2}$ fermions, possess no internal structure, and are considered fundamental particles. They come in three flavours —electron, muon, and tau— each corresponding to a different generation of leptons. Neutrinos have no electric or colour charge, making them interact exclusively through the weak nuclear force and gravity. The absence of electromagnetic or strong interactions make neutrinos notoriously difficult to detect and study. The weak force mediates processes such as nuclear decays and particle collisions by enabling the transformation of one type of particle into another or facilitating interactions via the exchange of W and Z bosons. Due to the weak force's extremely short range, approximately 10^{-18} meters, neutrinos can traverse enormous volumes of matter without interacting, as interactions occur only when a neutrino comes very close to a particle capable of mediating the interaction. The likelihood of a neutrino interacting with matter is quantified by its cross-section. For weak interactions, the cross-section can be estimated using the simplified expression,

$$\sigma \sim G_F^2 E_\nu^2 \tag{1}$$

where G_F is the Fermi coupling constant, which quantifies the strength of the weak interaction, and E_ν is the energy of the neutrino. However, the cross-section is typically measured experimentally rather than calculated, as it depends on various factors such as the type of interaction and the target material, making experimental data necessary to confirm theoretical models.

Massless or Massive?

Initially, neutrinos were thought to be massless due to principles of gauge symmetries and the Higgs mechanism. The Standard Model is grounded in gauge symmetries, with $SU(2)_L \times U(1)_Y$ being the key gauge group for electroweak interactions. The $SU(2)_L$ component of this gauge group implies that the weak interaction only affects left-handed doublets of particles (or right-handed doublets of antiparticles). Since neutrinos interact solely via the weak force, they should exist only as left-handed particles. On the other hand, the Higgs mechanism, which explains how particles acquire mass through spontaneous symmetry breaking, requires interactions between both left-handed and right-handed components of a particle via the Higgs field. The observation of only left-handed neutrinos and right-handed antineutrinos, combined with the necessity of both chiralities for mass acquisition via the Higgs field, led to the belief that neutrinos were massless.

However, in 1998, the Super-Kamiokande experiment observed neutrino oscillations in atmospheric neutrinos[2]. Neutrino oscillation is a phenomenon where a neutrino changes flavour as it travels, which can only occur if neutrinos have mass. This ground-breaking discovery necessitated a revision of the Standard Model, which had previously assigned neutrinos zero mass. As a result, various models, such as the seesaw mechanism, grew in popularity as explanations for how neutrinos acquire mass.

Neutrino Oscillations

Neutrinos are produced and detected in specific flavour states, which correspond to the charged lepton they are associated with in weak interactions: the electron $|\nu_e\rangle$, muon $|\nu_\mu\rangle$, and tau $|\nu_\tau\rangle$ neutrinos. Each flavour state is a superposition of mass states — a phenomenon known as neutrino mixing[8]. The mass states, denoted $|\nu_1\rangle, |\nu_2\rangle,$ and $|\nu_3\rangle$, represent neutrinos with definite masses m_1 , m_2 , and m_3 , and are eigenstates of the Hamiltonian describing the neutrino's free propagation. The relationship between flavour states $|\nu_\alpha\rangle$ (where $\alpha = e, \mu, \tau$) and mass states is described by the Pontecorvo-Maki-Nakagawa-Sakata (PMNS) matrix $U_{\alpha i}$:

$$|\nu_\alpha\rangle = \sum_{i=1}^{3} U_{\alpha i} |\nu_i\rangle \tag{2}$$

Because flavour states are surerpositions of mass states, when a neutrino travels through space, the mass states propagate with slightly different phases due to their distinct masses. This phase difference causes the superposition to evolve, which means that a neutrino can be detected in a different flavour state than the one in which it was initially produced. The probability P of a

neutrino oscillating from one flavour v_α to another flavour v_β after traveling a distance L with energy E if given by:

$$P\left(v_\alpha \to v_\beta\right) = \sin^2(2\theta)\sin^2\left(\frac{\Delta m^2 L}{4E}\right) \tag{3}$$

Here, θ is the mixing angle between the neutrino flavours, and $\Delta m^2 = m_i^2 - m^2$ represents the difference in the squared masses of the neutrino mass eigenstates. While this equation specifically applies to two-flavour mixing scenarios, a more general formula accounts for all possible neutrino flavours and mass states. This general equation involves summing over contributions from all mass eigenstate pairs and is applicable for describing oscillations involving more than two neutrino flavours:

$$P\left(v_\alpha \to v_\beta\right) = \delta_{\alpha\beta} - 4\sum_{i>j}\mathrm{Re}\left(U_{\alpha i}U^*_{\beta i}U^*_{\alpha j}U_{\beta j}\right)\sin^2\left(\frac{\Delta m^2_{ij}L}{4E_v}\right) \tag{4}$$

Where $\delta_{\alpha\beta}$ is the Kronecker delta, which equals 1 if $\alpha = \beta$ (indicating no oscillation) and 0 if $\alpha \neq \beta$ (indicating oscillation), and $U_{\alpha i}$ are the elements of the PMNS matrix.

There are three mixing angles θ_{12}, θ_{23}, and θ_{13}, each governing the mixing between the two mass states corresponding to its indices. These angles describe the degree of mixing between different neutrino flavours and mass states. The PMNS matrix if parameterised by these mixing angles, as well as one CP-violating phase δ_{CP}. The matrix can be expressed as:

$$U_{PMNS} = \begin{pmatrix} c_{12}c_{13} & s_{12}c_{13} & s_{13}e^{-i\delta_{CP}} \\ -s_{12}c_{23} - c_{12}s_{23}s_{13}e^{i\delta_{CP}} & c_{12}c_{23} - s_{12}s_{23}s_{13}e^{i\delta_{CP}} & s_{23}c_{13} \\ s_{12}s_{23} - c_{12}c_{23}s_{13}e^{i\delta_{CP}} & -c_{12}s_{23} - s_{12}c_{23}s_{13}e^{i\delta_{CP}} & c_{23}c_{13} \end{pmatrix} \tag{5}$$

Where $c_{ij} = \cos\theta_{ij}$ and $s_{ij} = \sin\theta_{ij}$. A key aspect of this matrix is that the CP-violating phase δ_{CP} allows for the possibility of CP violation in the lepton sector. This remains an active area of research, and the exact value of δ_{CP} is still unknown.

In summary, if neutrinos were massless, their flavour states would remain stable and no oscillations would be observed. The fact that neutrinos do oscillate indicates that their mass states evolve differently as they travel, causing changes in flavour composition over time. Thus, neutrino oscillations provide compelling evidence that neutrinos do indeed have mass.

Neutrino Mass

The first issue in understanding neutrino mass is the absence of a known mechanism to generate it. As previously discussed, the Higgs mechanism is the established process for giving mass to particles, which requires the presence of both left-handed and right-handed components[9]. However, only left-handed neutrinos have been observed, suggesting two possibilities: either undetected right-handed neutrinos exist, which would enable neutrino–Higgs Yukawa interactions and result in Dirac masses for the neutrino states, or an alternative mechanism is responsible for generating neutrino mass.

To further illustrate the necessity of both chiralities for mass generation, we can examine the Lagrangian for spin $\frac{1}{2}$ fields, which encompasses all fermions. The free Lagrangian for spinor fields, also known as the Dirac Lagrangian, can be written as:

$$\mathscr{L}_{\text{Free}} = (\mathrm{c})\bar{\Psi}\gamma^\mu\partial^\mu\Psi + mc^2\bar{\Psi}\Psi \tag{6}$$

Using $\Psi = (\Psi_L + \Psi_R)$, being Ψ_L the left and Ψ_R the right chiral part of the spinor, we can rewrite the Lagrangian in terms of the chiralities:

$$\mathscr{L}_{\text{Free}} = c\left[\bar{\Psi}_L\gamma^\mu\partial^\mu\Psi_L + \bar{\Psi}_R\gamma^\mu\partial^\mu\Psi_R\right] + mc^2\left[\bar{\Psi}_L\Psi_R + \bar{\Psi}_R\Psi_L\right] \tag{7}$$

We can see that while the kinetic term keeps the left-handed and right-handed components decoupled, the mass term links them together. This coupling implies that for spin $\frac{1}{2}$ fields to acquire mass, both chiralities must be present. The second challenge related to neutrino masses is their scale. While it is confirmed that neutrino masses are non-zero, they remain extraordinarily small. In contrast to the masses of charged fermions, which vary widely but are evenly distributed - spanning more than five orders of magnitude and including values on the order of $1, 10, 10^2, 10^3, 10^4$, and $10^5 \mathrm{MeV/c^2}$ - neutrino masses are several orders of magnitude smaller, falling below $10^{-6}\mathrm{MeV/c^2}$ (or $1\mathrm{eV/c^2}$). Furthermore, there are no known fundamental fermions with masses in the intermediate range between these scales. This stark difference underscores the unique nature of neutrinos compared to other particles. Consequently, any theoretical models must not only explain the existence of non-zero neutrino masses but also address why these masses are so exceptionally small.

The third challenge is measuring neutrino masses. Given their incredibly small mass, which is below the sensitivity of most direct measurement techniques, determining their exact values is highly challenging. This difficulty is compounded by their weak interactions with matter, which make them hard to detect. Despite not knowing the absolute mass scale of neutrinos (i.e., the exact values $\mathrm{pf_f} m_1, m_2$ and m_3), it is possible to measure the differences in the squares of their masses through neutrino oscillation experiments[10]. The mass-squared difference between the first (v_1) and second (v_2) mass states is denoted by $\Delta m^2_{21} \approx 7.42 \times 10^{-5}\mathrm{eV}^2$. The difference between the mass-squared of the third mass state (v_3) and either the first or second mass states is given by $\Delta m^2_{31} \approx 2.517 \times 10^{-3}\mathrm{eV}^2$, for the normal hierarchy, or $\Delta m^2_{32} \approx -2.497 \times 10^{-3}\mathrm{eV}^2$, for the inverted hierarchy. These measurements reveal another uncertainty - the mass hierarchy which indicates the ordering of the neutrino mass eigenstates. In the normal hierarchy scenario, v_1 is the lightest, v_2 is heavier and v_3 is the heaviest, corresponding to $m_1 < m_2 < m_3$. This hierarchy is analogous to the mass ordering of other fermions in the Standard Model, where masses

increase with each generation. In contrast, the inverted hierarchy scenario suggests that v_3 is the lightest, while v_1 and v_2 are heavier, corresponding to $m_3 < m_1 < m_2$. Determining the exact mass hierarchy is crucial for understanding neutrino mass generation theories. Lastly, there are constraints on the sum of neutrino masses, $\sum m_v = m_1 + m_2 + m_3$. Cosmological data [11] suggest that this sum is less than about 0.12 eV ($\sum m_v < 0.12eV$). For the normal hierarchy, the minimum sum is approximately 0.06 eV, while for the inverted hierarchy, it is about 0.1 eV.

Finally, there are three main types of models proposed to address the problem of neutrino masses:

1. Adding particles – This approach involves introducing new chiral fermions into the Standard Model. These additional particles enable neutrinos to interact with the Higgs field, thereby generating mass.

2. Allowing other sources of electroweak symmetry breaking – This model suggests the inclusion of an additional Higgs boson that contributes specifically to neutrino masses without affecting the masses of other particles. This approach aims to maintain the overall symmetry-breaking mechanism of the Standard Model while accommodating neutrino mass generation.

3. Adding new sources of mass – These models propose that neutrino masses originate from a combination of the electroweak symmetry-breaking scale and a distinct, independent mass scale. In this scenario, neutrino masses would have a dual origin, influenced by both the known electroweak scale and a new, unexplored mass scale.

Despite the variety of approaches, the leading theoretical framework fits into the first category, and involves the introduction of heavy right-handed neutrinos. The Seesaw Mechanism, which will be explored in detail in the following section, provides a foundational understanding for the rest of this paper.

The Seesaw Mechanism

The seesaw mechanism is a theoretical framework that addresses the smallness of neutrino masses. In the Type I seesaw mechanism [12], which we will focus on, right-handed neutrino singlets, often called "sterile neutrinos" as they do not interact via the Standard Model interactions, are introduced. This type involves both Dirac and Majorana mass terms. Type II introduces a new Higgs triplet scalar field which couples directly to the left-handed neutrino doublets. This triplet Higgs field acquires a small vacuum expectation value (VEV), which directly gives mass to the left-handed neutrinos. Type III uses heavy fermion triplets that transform as a triplet under the $SU(2)_L$ gauge group. The mass term in this case involves a Yukawa coupling between the left-handed lepton doublets, the fermion triplets, and the Higgs doublet. This mechanism has a structure similar to that of type I, as it also results in one light neutrino and one heavy neutrino. To summarise:

- Type I: Involves singlet fermions under $SU(3) \times SU(2) \times U(1)$
- Type II: Involves triplet scalars under $SU(2)$
- Type III: Involves triplet fermions under $SU(2)$

Type 1

In a type 1 seesaw model, two distinct mass terms are allowed in the electroweak Lagrangian. The Dirac mass term

$$-m_D\left(\overline{v_L}v_R + \overline{v_R}v_L\right) \tag{8}$$

and the Majorana mass term,

$$-\frac{1}{2}m_M^L\left(\bar{v}_L v_L^c + \bar{v}_L^c v_L\right) - \frac{1}{2}m_M^R\left(\bar{v}_R v_R^c + \bar{v}_R^c v_R\right) \tag{9}$$

The Dirac mass term links the left-handed and right-handed components of a neutrino, whereas the Majorana mass term couples a neutrino to its charge conjugate, suggesting that the neutrino is mass term violates lepton number by two units. Both mass terms can be represented in a mass matrix $\mathscr{M}$, which combines their contributions:

$$\mathscr{M} = \begin{pmatrix} m_M^L & m_D \\ m_D & M_M^R \end{pmatrix} \tag{10}$$

This matrix captures all couplings as m_M^L is the left-handed Majorana mass term (coupling v_L with v_L^c), M_M^R is the right-handed Majorana term (coupling v_L with V_R^c), and m_D is the Dirac mass term (compling v_L with v_R and vise versa). By using this matrix, both mass terms can be expressed as a single Lagrangian mass term, written as

$$\mathscr{L}_{\text{mass term}} = -\frac{1}{2}\left(\bar{v}_L, \bar{v}_R^c\right)\mathscr{M}\begin{pmatrix} v_L^c \\ v_R \end{pmatrix} + h.\text{c.} \tag{11}$$

In order to address the question of why neutrino masses are so small, we diagonalize the mass matrix, moving to the mass basis, where we obtain two mass eigenstates with eigenvalues m_v and M. In this case, the mass matrix is given by:

$$\mathscr{M}' = \begin{pmatrix} m_v & 0 \\ 0 & M \end{pmatrix} \tag{12}$$

The corresponding Lagrangian mass term would then be:

$$\mathscr{L}_{\text{mass term}} = -\frac{1}{2}(\bar{\nu}\bar{N})\mathscr{M}'\begin{pmatrix} \nu \\ N \end{pmatrix} + h.c. \tag{13}$$

Where ν and N are the fields coupled to the Higgs, corresponding to the mass eigenvalues m_v and M, respectively. Thus, ν and N represent the mass eigenstates of the neutrinos, while

ν_L and ν_R, which are the states observed in weak interactions, are linear superpositions of v and N.

The seesaw mechanism takes $m_v = 0$, implying that v is decoupled from the Higgs field. Returning to the mass matrix $\mathscr{M}$, the characteristic equation is given by:

$$\left(m_M^L - \lambda\right)\left(m_M^{\mathrm{R}} - \lambda\right) - (m_D)^2 = 0 \tag{14}$$

Whose solutions for the eigenvalues λ of the mass matrix M are given by:

$$\lambda_{\pm} = \frac{1}{2}\left(m_M^L + m_M^R\right) \pm \sqrt{\frac{1}{4}\left(m_M^L + m_M^R\right)^2 + m_M^L m_M^R - m_D^2} \tag{15}$$

From these solutions, we find that:

$$\lambda_{-} = m_v = 0$$
$$\lambda_{+} = M = m_M^L + m_M^R \tag{16}$$

Additionally, by maintaining $\lambda_{-} = 0$, we obtain:

$$m_M^L m_M^R = m_D^2 \tag{17}$$

Which implies that the Dirac mass m_D is the geometric mean of the left and right-handed Majorana masses. Furthermore, given a fixed value of m_D, this equation indicates that increasing m_M^R leads to a decrease in m_M^L. It is this inverse relationship that gives the seesaw mechanism its name. Finally, if we express the eigenvectors v (for λ_{-}) and N (for λ_{+}) in the ν_L and ν_R basis, we get:

$$N = (\nu_R + \nu_R^c) + \frac{m_D}{m_M^R}(\nu_L + \nu_L^c) \tag{18}$$

$$v = (\nu_L + \nu_L^c) + \frac{m_D}{m_M^R}(\nu_R + \nu_R^c) \tag{19}$$

If we now assume that

$$m_M^R \gg m_D \tag{20}$$

then N is predominantly composed of ν_R, and vice versa, implying that ν_R is very heavy and effectively behaves as a sterile neutrino. Similarly, ν_L is almost entirely composed of the weightless ν, making it extremely light. Additionally, the larger m_M^R is, the more ν_R approaches N and ν_L approaches v.

If condition (20) holds, then from the equation (17) we can conclude that

$$m_M^L \approx 0(\text{ but } \neq 0) \tag{21}$$

And from equation (16) we can derive that:

$$m_M^R \approx M \tag{22}$$

This results in a mass hierarchy that aligns with the experimental observations and is supported by a strong theoretical framework, where heavy sterile right-handed neutrinos balance the small mass of left-handed neutrinos

$$M \approx m_M^R \gg m_D > m_M^L \approx 0 \tag{23}$$

Regarding the nature of neutrinos, although the seesaw mechanism interplays both Dirac and Majorana mass terms, the presence of the Majorana term suggests that neutrinos are Majorana particles, that is, their own antiparticles. If neutrinos were Dirac particles, the Majorana mass term would violate gauge symmetry, ruling out that possibility. Therefore, observing neutrinos as Majorana particles would provide compelling evidence for the seesaw mechanism's role in generating neutrino masses.

Matter-Antimatter Asymmetry

The prediction of antimatter emerged as a direct result of combining two of the most fundamental concepts in physics: relativity and quantum mechanics. Dirac brought these concepts together in his famous equation, which intriguingly yielded two distinct solutions [13]. These solutions were eventually interpreted to mean that a corresponding antiparticle exists for every particle. The subsequent detection of antimatter a few years later [14] confirmed this hypothesis and posed an amazing success for theoretical physics. Antimatter was then considered to be analogous to matter but with opposite charges and quantum numbers. Since all phenomena observed at that time were invariant under parity (P), charge conjugation (C), and time reversal (T), the scarcity of antimatter in the nearby universe lead to the belief that the universe was created with different amounts of matter and antimatter.

However, with the rise of the Big Bang theory [15,16] and the observational discovery of cosmic microwave background (CMB) [17], it became evident that the high-energy conditions in the early universe should have produced matter and antimatter in symmetric quantities. Antimatter was present when the pair production and annihilation processes were in thermal equilibrium in the first seconds of the Universe. When the particle energies became too small for pair creation as a result of the cooling plasma, almost all particles and antiparticles were annihilated, leaving a small amount of matter. The mechanisms that produced this asymmetry remain uncertain.

Baryon Asymmetry

The observed matter-antimatter asymmetry is intrinsically linked to baryon asymmetry. Baryons, such as neutrons and protons, constitute the majority of the visible matter in the universe. Therefore, any deviation from the matter-antimatter balance is reflected in an asymmetry between baryons and antibaryons. The baryon asymmetry of the universe (BAU) can be estimated

by the baryon asymmetry parameter η

$$\eta = \frac{nB - n\bar{B}}{n\gamma} \tag{24}$$

where $nB, n\bar{B}$, and $n\gamma$ are the number densities of baryons, antibaryons, and photons, respectively.

There are two separate ways of determining this baryon to photon ratio. Big Bang nucleosynthesis (BBN) processes, which are responsible for the formation of light elements, start around T $\lesssim$ 1MeV when neutrino interactions slow down compared to the universe's expansion [18]. Given the well-understood particle physics at this stage, η can be determined by measuring the primordial abundances of light elements. The result found in [19] is $\eta_{BBN} = (6.10 \pm 0.04) \times 10^{-10}$. The baryon content of the universe can also be determined from the power spectrum of temperature fluctuations in the (CMB). These fluctuations arose from acoustic oscillations of the baryon-photon plasma in dark matter's gravitational potential. The oscillations are sensitive to η, affecting the plasma's equation of state and the relative height of peaks in the power spectrum. This provides an independent measurement of η since it involves different physics and occurs at a much later epoch (T $\sim$ 0.3eV) than BBN. The Planck 2018 data [11] give $\eta_{CMB} = (6.13 \pm 0.03) \times 10^{-10}$ (derived from the baryon density parameter $\Omega_b h^2 = 0.0224 \pm 0.0001$).

The empirical values obtained from both methods (BBN and CMB analysis) are in agreement, consistently giving values $\sim 6 \times 10^{-10}$, supporting the theoretical framework. This value provides a measurable way to quantify the imbalance between baryons and antibaryons, as a high baryon to photon ratio indicates a significant excess of baryons over anti-baryons.

Sakharov Conditions

In 1967 Sakharov proposed three conditions necessary to obtain baryon asymmetry [20]. These are baryon number violation, C and CP violation, and interactions out of thermal equilibrium. The reason why each condition must be obeyed is reasonably intuitive.

The baryon number is a conserved quantum number defined as $B = \frac{1}{3}(n_q - n_{\bar{q}})$, representing the difference between the number of quarks (n_q) and antiquarks $(n_{\bar{q}})$. Since the early universe produced equal amounts of matter and antimatter, initially $B = 0$. Naturally, without baryon number violation, it is impossible for a system to evolve from a $B = 0$ state to one with $B \neq 0$.

Regarding the second condition, the charge conjugation operator, C , flips all internal quantum numbers, that is, transforms a particle into its antiparticle $C : Q \to -Q$. The parity operator, P , reverses spatial coordinates, essentially turning a system into its mirror image $P : X \to -X$. CP transformations change both the charge and the chirality of a particle $CP : q_L \to \bar{q}_R$. Since CP symmetry would equally favour the processes that create matter and antimatter, it must be violated. We shall look into CP violation mechanisms in the following section.

Finally, a system in thermal equilibrium is in a time translation invariant state in which the expectation values of all measurable quantities remain unchanged. That is, forward and reverse processes occur at the same rate, preventing the generation of any asymmetries: $\Gamma(X \to Y) = \Gamma(Y \to X)$. Therefore, it requires a departure from thermal equilibrium to allow for the baryon-violating and CP -violating processes to create an imbalance.

CP violation in the Standard Model

As explained earlier, CP symmetry must be violated to account for the observed imbalance between matter and antimatter. There are two primary mechanisms for CP violation: one in the strong interaction and one in the electroweak interaction. Additionally, various other mechanisms exist in extensions of the Standard Model.

The Strong CP problem

Quantum Chromodynamics (QCD) is the theory that describes the strong interaction, which governs the interactions between quarks and gluons. The QCD Lagrangian, encapsulating the dynamics of these particles, is expressed as

$$\mathscr{L}_{QCD} = -\frac{1}{4} F^{\alpha}_{\mu\nu} F^{\alpha\mu\nu} + \sum_f \bar{q}_f \left(i\gamma^\mu D_\mu - m_f \right) q_f \tag{25}$$

This Lagrangian is primarily CP-conserving, consistent with the expectation that the strong force conserves CP symmetry. However, it was soon recognised that the theory allows for an additional parameter, the θ parameter, associated with an extra term in the Lagrangian [21]. Known as the θ-term, this term can violate CP symmetry. θ is a dimensionless parameter that takes values between 0 and 2π, determining the strength of CP violation in the strong interaction. The θ-term can thus be written as:

$$\mathscr{L}_\theta = \theta \frac{1}{16\pi^2} F^{\alpha}_{\mu\nu} \tilde{F}^{\mu\nu\alpha} \tag{26}$$

where $\tilde{F}^{\alpha}_{\mu\nu} = \frac{1}{2} \varepsilon_{\mu\nu\rho\sigma} F^{\rho\sigma\alpha}$, with $\varepsilon_{\mu\nu\rho\sigma}$ being the Levi-Civita symbol. The θ-term introduces CP violation in QCD through its violation of time-reversal (T) symmetry. The field strength tensor $F^{\alpha}_{\mu\nu}$ includes first-order time derivatives of the gauge fields. When $F^{\alpha}_{\mu\nu}$ is contracted with its dual, $\tilde{F}^{\mu\nu\alpha}$, the resulting term retains its first-order nature with respect to time derivatives. Under a time-reversal transformation $(t \to -t)$, these time derivatives change sign, causing the θ-term to flip its sign. This explicit violation of T-symmetry implies a violation of CP symmetry, as preserving CPT invariance necessitates that breaking time-reversal symmetry also breaks CP symmetry.

One of the physical consequences of a non-zero θ-term is the generation of an electric dipole moment (EDM) in various

particles[22]. An EDM measures the separation of positive and negative charges within a particle. For the neutron, a non-zero EDM would indicate a preferred spatial orientation, signalling CP violation. The estimated magnitude of the neutron EDM, d_n, can be obtained through dimensional analysis:

$$d_n = e\frac{\theta m_q}{M_{QCD}^2} \tag{27}$$

where m_q is a light quark mass, and $M_{QCD} \sim 200\text{MeV}$ is the characteristic QCD energy scale. The suppression by M_{QCD}^2 arises because the EDM is generated at the nonperturbative QCD scale rather than directly at the Lagrangian level. Experimental measurements of the neutron EDM[23] set an extremely small upper bound of approximately $d_n < 10^{-26}\text{e}\cdot\text{cm}$, placing a very stringent constraint on $\theta : \theta \lesssim 10^{-10}$. This unexpectedly small value for θ is surprising because one might intuitively expect it to be of order 1. This discrepancy highlights the "Strong CP Problem", which underscores that strong CP violation alone cannot account for the matter-antimatter asymmetry observed in the universe.

CP violation in the Electroweak Sector

While the strong CP problem poses a significant puzzle within the framework of QCD, CP violation in the weak interaction is well-established[24]. In the Standard Model, the primary source of CP violation in the weak sector originates from the Cabibbo-Kobayashi-Maskawa (CKM) matrix. The CKM matrix, denoted as V_{CKM}, is a 3×3 unitary matrix that connects the weak interaction eigenstates of quarks to their mass eigenstates. The elements V_{ij} of this matrix represent the probability amplitude for a transition from a quark of type i to a quark of type j.

$$V_{CKM} = \begin{pmatrix} V_{ud} & V_{us} & V_{ub} \\ V_{cd} & V_{cs} & V_{cb} \\ V_{td} & V_{ts} & V_{tb} \end{pmatrix} \tag{28}$$

Here, u, c, and t denote the up-type quarks, while d, s, and b denote the down-type quarks. A key aspect of the CKM matrix in relation to CP violation is its inclusion of a complex phase. This complex phase can result in differing probabilities for processes and their CP-conjugate counterparts when quark transitions involve the CKM matrix elements. The other phases in V_{CKM} that do not contribute to physical CP violation can be removed by rephasing the quark fields. The degree of CP violation is quantified by the Jarlskog invariant, J , which is expressed as:

$$J = \text{Im}\left(V_{ud}V_{cs}V_{us}^*V_{cd}^*\right) \tag{29}$$

This quantity remains invariant under phase redefinitions, meaning it represents a physically meaningful measure of CP violation rather than an arbitrary phase choice. Its nonzero value ensures CP violation in the weak interaction, but its small numerical value explains why the observed baryon asymmetry is much larger than what Standard Model CP violation can produce.

Experimental observations of CP violation have been made in the decays of kaons[25], B-mesons[26], and D-mesons[27]. The differences in the decay rates of K^0 and $\bar{K}^0$ into specific final states are direct manifestations of the complex phase in the CKM matrix.

Lack of CP violation

We have identified two mechanisms for CP violation, but they fall short of explaining the observed baryon asymmetry. The BAU is estimated to be around $\eta \approx 10^{-10}$[28]. The CP violation attributable to the CKM matrix can only account for an asymmetry on the order of 10^{-20}, which is many orders of magnitude smaller than what is needed. This suppression arises from the hierarchical structure of quark masses and the smallness of the Jarlskog invariant, which limits the effectiveness of sphaleron transitions in generating a sufficient asymmetry. For the strong force, the potential CP violation could come from the θ-term, but experimental limits on the neutron EDM require $\theta \lesssim 10^{-10}$. Thus, any CP violation from the strong sector is also negligible.

Since neither the weak nor strong CP violation mechanisms are sufficient, additional sources of CP violation beyond the Standard Model are necessary. One promising candidate is leptogenesis, which involves CP violation in the lepton sector. This CP violation could create an asymmetry in the lepton number, which could then be converted into a baryon asymmetry in the early universe.

Leptogenesis

Leptogenesis simultaneously addresses the problems of neutrino masses and CP violation. First proposed by Mikhail Shaposhnikov in 1985[29], leptogenesis represents a significant shift from earlier theories that focused exclusively on baryogenesis. The foundational paper "Baryogenesis Without Grand Unification"[30] established the connection between the decay of heavy right-handed neutrinos and lepton asymmetry, laying the groundwork for the current mechanism.

Leptogenesis suggests that in the early universe, certain interactions involving heavy right-handed neutrinos violate both CP symmetry and lepton number conservation. These violations create an excess of leptons over antileptons. Sphaleron processes can convert the initial lepton asymmetry into a baryon asymmetry, ultimately leading to the observed dominance of matter over antimatter in the universe. This mechanism not only explains the origin of baryon asymmetry but also links it to the physics of neutrinos, making leptogenesis a compelling framework in both cosmology and particle physics.

Decay of Right-Handed Neutrinos

The right-handed neutrinos were introduced by the seesaw mechanism as an extension of the Standard Model to explain neutrino masses. These play a pivotal role in Leptogenesis as it is their decay that violates lepton number and CP symmetry, producing an excess of leptons over antileptons.

Decay process

Depending on the mass and mixing parameters, right-handed neutrinos (N_R) can decay through various channels, mediated by both charged (W_R) and neutral (Z) gauge bosons, as well as Higgs bosons[31]. The dominant decay modes are typically:

1. Decays involving Higgs bosons, where a right-handed neutrino decays into a light neutrino and a Higgs boson:

$$N_R \to \nu + H \tag{30}$$

   In scenarios where the right-handed neutrinos are very massive, decays into Higgs bosons become kinematically accessible. Subsequent decays of the Higgs boson could produce additional jets or leptons, contributing to complex final states.

2. Neutral current decays via Z bosons, where the heavy neutrino decays into a light neutrino and a Z boson, which further decays into pairs of charged leptons, neutrinos, or jets:

$$N_R \to \nu + Z \to \nu + jj\left(\text{ or } \ell^+\ell^- \text{or } \nu\bar{\nu}\right) \tag{31}$$

   This channel contributes to signatures with missing transverse energy (due to neutrinos) and dilepton or dijet pairs, depending on the decay products of the Z boson. The decay of the heavy neutrino can be represented by the diagram:

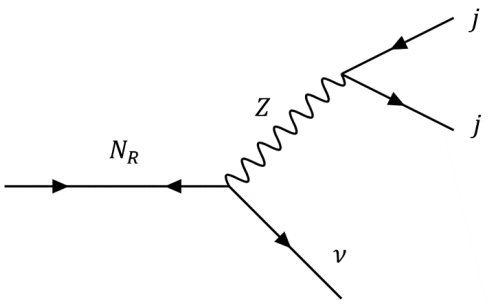

Fig. 1 Feynman diagram illustrating the decay process of a heavy right-handed neutrino into a light neutrino and a dijet mediated by Z boson exchange.

3. Charged current decays via W_R bosons, where right-handed neutrinos decay into a charged lepton (ℓ) and a virtual W_R boson, which subsequently decays into two jets (hadronic decay) or a pair of leptons (leptonic decay):

$$N_R \to \ell^\pm + W_R^\mp \to \ell^\pm + jj\left(\text{ or } \ell^\mp \nu\right) \tag{32}$$

   The Majorana nature of N_R allows it to decay into both a lepton and antilepton final state, which can lead to same-sign dilepton events, violating lepton number. This process can be depicted by the following diagram:

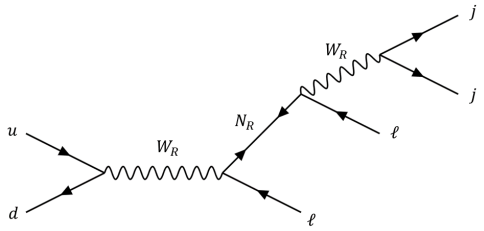

Fig. 2 Feynman diagram depicting the production of a heavy right-handed neutrino and its subsequent decay into a dilepton and a dijet via W_R boson exchange.

   Here, W_R is a hypothetical gauge boson that interacts with right-handed fermions, in contrast to the standard W boson of the Standard Model which interacts with left-handed fermions. It is worth noting, however, that the right-handed neutrinos in the Type I seesaw mechanism are singlets under the Standard Model gauge group and do not couple to W_R bosons. Thus, this channel is not possible unless the seesaw model is extended to include new gauge bosons, like in Left-Right Symmetric Models[32].

Decay Width

Generally, the decay widths of right-handed neutrinos in the Type I seesaw are suppressed by the small mixing angles between the right-handed and the left-handed neutrinos, represented by parameters like $\theta = \frac{m_D}{M_{N_R}}$. Consequently, decay widths involving right-handed neutrinos are typically very small unless M_{N_R} is close to the electroweak scale.

The decay width of a heavy right-handed neutrino decaying via a Higgs, Z , or W boson can be expressed as[33]:

$$\Gamma(N_R \to \nu + H) = \frac{g^2}{64\pi} |V_{\ell N_R}|^2 \frac{M_{N_R}^3}{M_W^2} \left(1 - \frac{m_H^2}{M_{N_R}^2}\right)^2 \tag{33}$$

$$\Gamma(N_R \to \nu + Z) = \frac{g^2}{64\pi c_W^2} |V_{\ell N_R}|^2 \frac{M_{N_R}^3}{M_Z^2} \left(1 - \frac{m_Z^2}{M_{N_R}^2}\right) \left(1 + \frac{m_Z^2}{M_{N_R}^2} - 2\frac{m_Z^4}{M_{N_R}^4}\right) \tag{34}$$

$$\Gamma(N_R \to \ell + W) = \frac{g^2}{64\pi} |V_{\ell N_R}|^2 \frac{M_{N_R}^3}{M_W^2} \left(1 - \frac{m_W^2}{M_{N_R}^2}\right)^2 \left(1 + \frac{m_W^2}{M_{N_R}^2} - 2\frac{m_W^4}{M_{N_R}^4}\right) \tag{35}$$

where $V_{\ell N_R}$ is the small mixing $|V_{\ell N_R}|^2 \sim 10^{-3} - 10^{-4}$.

Breaking CP Symmetry

For leptogenesis to occur, CP symmetry must be violated in the decays of the right-handed neutrinos. CP violation is essential because it allows for a difference in the rates of decay for a particle and its antiparticle, leading to an excess of leptons over antileptons. We shall analyse how CP violation arises in each decay channel and how these contributions combine to produce an overall CP asymmetry [34].

CP Violation in Higgs-Mediated Decays

The CP violation in these decays arises from the interference between tree-level decays and one-loop diagrams involving the exchange of another heavy right-handed neutrino:

- The tree-level decay is the simplest decay process, where N_i decays directly to a lepton and a Higgs boson
- The one-loop vertex correction is a one-loop diagram where the decay product Higgs and lepton recombine via a vertex correction involving another heavy neutrino N_j
- The one-loop self-energy correction is a one-loop diagram where the neutrino N_i oscillates into another neutrino N_j before decaying, altering the effective decay amplitude

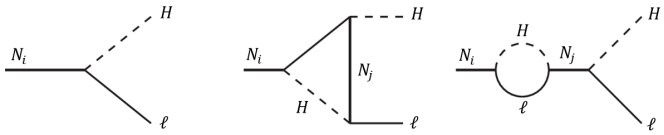

Fig. 3 Feynman diagrams illustrating Higgs-mediated decay processes of a heavy right-handed neutrino N_i. (Left) Tree-level decay of N_i into a lepton and a Higgs boson. (Middle) One-loop vertex correction involving the exchange of a second heavy neutrino N_j, a lepton, and a Higgs boson. (Right) One-loop self-energy correction where N_i decays into N_j with a virtual lepton and Higgs boson in the loop, followed by the subsequent decay of N_j. These processes include CP-violation due to the quantum interference between the tree-level diagram and the radiative corrections.

The CP asymmetry parameter for Higgs-mediated decays is defined as:

$$\varepsilon_i^H = \frac{\Gamma(N_i \to \nu_\alpha H) - \Gamma(N_i \to \bar{\nu}_\alpha \bar{H})}{\Gamma(N_i \to \nu_\alpha H) + \Gamma(N_i \to \bar{\nu}_\alpha \bar{H})} \tag{36}$$

This asymmetry can be expressed as:

$$\varepsilon_i^H = \frac{1}{8\pi (y^\dagger y)_{ii}} \sum_{j \neq i} \mathrm{Im}\left[(y^\dagger y)_{ij}^2\right] \left(f\left(\frac{M_j^2}{M_i^2}\right) + g\left(\frac{M_j^2}{M_i^2}\right)\right) \tag{37}$$

Where y are the Yukawa couplings of the neutrinos to leptons and Higgs, and $f(x)$ and $g(x)$ are loop functions associated with vertex and self-energy corrections, respectively. For Higgs-mediated decays, their typical forms are:

$$f(x) = \sqrt{x}\left(1 - (1+x)\ln\left(\frac{1+x}{x}\right)\right) \tag{38}$$

$$g(x) = \frac{\sqrt{x}}{1-x} \tag{39}$$

CP Violation in Z-Mediated Neutral Current Decays

Similar to Higgs-mediated decays, CP violation in Z-mediated decays arises from the interference between tree-level decays and one-loop corrections:

- In the tree-level decay N_i decays directly to a neutrino and a Z boson
- The one-loop corrections involve virtual particles, such as another heavy neutrino N_j that can interfere with the tree-level process

The CP asymmetry parameter for Z-mediated decays is given by:

$$\varepsilon_i^Z = \frac{\Gamma(N_i \to \nu_\alpha Z) - \Gamma(N_i \to \bar{\nu}_\alpha Z)}{\Gamma(N_i \to \nu_\alpha Z) + \Gamma(N_i \to \bar{\nu}_\alpha Z)} \tag{40}$$

The expression for ε_i^Z is similar to ε_i^ϕ but with different loop functions. For Z-mediated decays, the loop functions $f_Z(x)$ and $g_Z(x)$ have analogous forms to $f(x)$ and $g(x)$, but differ slightly due to the different nature of the Z-boson interactions compared to Higgs interactions.

CP Violation in W_R-Mediated Charged Current Decays

Just like the Higgs-mediated and Z-mediated decays, CP violation in the W_R-mediated decays comes from the interference between tree-level decay amplitudes and one-loop corrections, and the asymmetry parameter is defined as:

$$\varepsilon_i^{W_R} = \frac{\Gamma\left(N_i \to \ell_\alpha^+ W_R^-\right) - \Gamma\left(N_i \to \ell_\alpha^- W_R^+\right)}{\Gamma\left(N_i \to \ell_\alpha^+ W_R^-\right) + \Gamma\left(N_i \to \ell_\alpha^- W_R^+\right)} \tag{41}$$

The $\varepsilon_i^{W_R}$ expression has the exact same form as ε_i^Z and ε_i^ϕ, where $f_{W_R}(x)$ and $g_{W_R}(x)$ are loop functions specific to charged current decays involving W_R bosons.

Combined CP Asymmetry with All Decay Channels

When considering all three decay channels, the total CP asymmetry ε_i for the decay of a heavy right-handed neutrino N_i is a weighted sum of the individual asymmetries:

$$\varepsilon_i = \frac{\Gamma_i^H \varepsilon_i^H + \Gamma_i^Z \varepsilon_i^Z + \Gamma_i^{W_R} \varepsilon_i^{W_R}}{\Gamma_i^H + \Gamma_i^Z + \Gamma_i^{W_R}} \tag{42}$$

Where Γ_i^H, Γ_i^Z and $\Gamma_i^{W_R}$ are the total decay widths for each respective decay.

There are three main factors that influence the overall strength of the CP violation. The interplay of the Yukawa couplings y_{ij} and their complex phases dictate the size of the imaginary parts that drive CP violation. The relative masses of the heavy neutrinos M_i affect the loop functions and therefore the magnitude of the CP asymmetry. Finally, the branching ratios of the decays into different channels determine how much each channel contributes to the overall CP asymmetry.

Connection to the Seesaw Mechanism

The connection between the seesaw parameters and CP violation in leptogenesis arises through the Yukawa matrix Y_D. The Dirac mass term m_D is related to the Yukawa couplings by $m_D = Y_D v$, where v is the Higgs vacuum expectation value. Since the seesaw formula for the light neutrino mass is:

$$m_\nu \approx -m_D M_M^{R^{-1}} {m_D}^T \tag{43}$$

substituting $m_D = Y_D v$, we obtain:

$$m_\nu \approx -Y_D v M_M^{R^{-1}} (Y_D v)^T \tag{44}$$

This explicitly shows how the Yukawa matrix Y_D is linked to the seesaw mechanism and the light neutrino masses. For leptogenesis, CP asymmetry is also expressed in terms of Yukawa couplings, as seen in equation (37). The Yukawa matrix can be rewritten in the Casas-Ibarra parametrization:

$$Y_D = \frac{\sqrt{M_M^R} R \sqrt{m_\nu} U^\dagger}{v} \tag{45}$$

where R is a complex orthogonal matrix, and U is the PMNS matrix. The CP-violating phases in U contribute to leptogenesis by influencing the decay asymmetry via Y_D. Since m_ν is experimentally constrained (by $0\nu\beta\beta$ and cosmology), this limits Y_D, which in turn constrains the possible values of ε_i^H. If the Majorana phases are small, the CP asymmetry is suppressed, affecting the viability of leptogenesis.

Baryogenesis via Leptogenesis

In the Standard Model, at very high temperatures (above the electroweak scale, $T \gtrsim 100\text{GeV}$), there exist special, non-perturbative solutions to the field equations of electroweak theory called sphalerons. They correspond to large, complex configurations of the electroweak fields and represent unstable saddle points in the energy landscape that connect neighboring vacua with different Chern-Simons numbers [35].

Sphaleron processes involve transitions between vacua with different baryon and lepton numbers, resulting in violations of both numbers. The change in the Chern-Simons number by one unit leads to a simultaneous violation of baryon and lepton numbers by an amount $\Delta B = \Delta L = 3$. This is due to the sphaleron's interaction with all three generations of quarks and leptons. As a result, sphaleron processes alter both baryon and lepton numbers together by the same amount, thus violating $B+L$ but conserving $B-L$.

In the context of leptogenesis, sphaleron processes are crucial because they can convert a lepton asymmetry into a baryon asymmetry [36]. When leptogenesis generates an excess of leptons, sphalerons can partially transform this excess into a baryon number, effectively creating baryon asymmetry. This relationship can be roughly described by $B \sim \frac{1}{3}(B-L)$. However, it is important to note that if leptogenesis results in a net $B-L$ asymmetry, sphalerons will conserve this quantity. Therefore, $B-L$ might be non-zero even if the initial state had $B-L=0$.

At these high temperatures, the Higgs field's vacuum expectation value goes to zero, restoring the full electroweak $SU(2)_L \times U(1)_Y$ symmetry. In this symmetric phase, sphalerons are unsuppressed and can efficiently convert any existing lepton asymmetry into a baryon asymmetry. The high energy and thermal fluctuations in the early universe can provide the system with enough energy to overcome the sphaleron energy barrier, leading to baryon and lepton number-violating transitions.

As the universe cools and undergoes the electroweak phase transition (EWPT), the sphaleron processes become suppressed [37]. If the EWPT is first-order, the symmetry breaking occurs abruptly, increasing the energy barrier for sphaleron transitions and effectively suppressing them. However, if the EWPT is second-order or a smooth crossover, additional mechanisms are required to suppress sphaleron processes. These might include the presence of new particles or interactions beyond the Standard Model, or simply the growing sphaleron energy barrier as the universe cools. In either case, once sphaleron processes are suppressed, any baryon asymmetry generated during the high-temperature phase is preserved. This asymmetry accounts for the dominance of matter over antimatter that we observe in the universe today.

In summary, if an initial lepton asymmetry is generated by some mechanism, such as leptogenesis, sphalerons can convert a portion of this lepton asymmetry into a baryon asymmetry.

This mechanism provides a natural explanation for the baryon asymmetry observed in the universe, with the resulting baryon asymmetry being of the same order of magnitude as the observed asymmetry ($\eta \approx 10^{-10}$).

Experimental Evidence Supporting Leptogenesis

Neutrinoless Double β-decay

Double beta decay is a process in which two neutrons within a nucleus simultaneously decay into two protons, two electrons, and two neutrinos. Neutrinoless double beta decay ($0\nu\beta\beta$) is a theoretical nuclear process in which the same transformation occurs, but without emitting any neutrinos, implying that the neutrinos involved annihilated each other. Although this occurrence would be extremely rare, its detection would provide direct evidence that neutrinos are Majorana particles, supporting the seesaw mechanism. Furthermore, as majorana particles violate lepton number in their interactions and lepton number violation is a necessary condition for leptogenesis, evidence of $0\nu\beta\beta$ would lend support to this mechanism. Additionally, detecting neutrinoless double beta decay could have implications for many other theories beyond the Standard Model, such as supersymmetry and grand unified theories.

Mechanism

Starting with conventional double beta decay, it can be represented as:

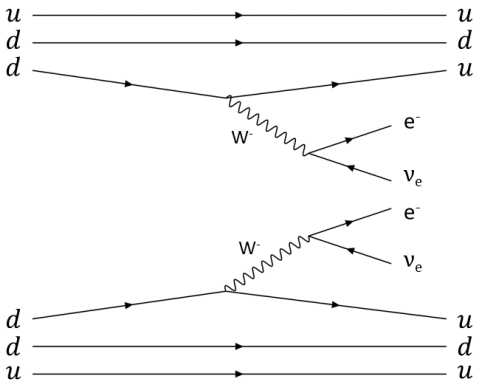

Fig. 4 Feynman diagram illustrating double beta decay $2\nu\beta\beta$. The diagram represents the transformation of a neutron into a proton, accompanied by the emission of two electrons and two neutrinos.

If these decays occur very close together in time, the emitted neutrinos could, in theory, annihilate each other:

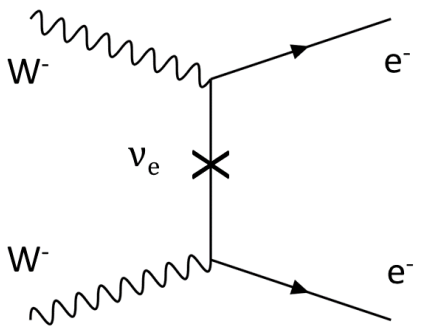

Fig. 5 Feynman diagram depicting the annihilation of neutrinos in neutrinoless double beta decay $0\nu\beta\beta$.

In this case, two neutrons decay into two protons and only two electrons, violating lepton number.

Experiments

Since the early 1980s, numerous experiments have been developed to detect the rare nuclear process of double beta decay. The choice of element used in these experiments is crucial, as many factors, such as the nuclear matrix elements, natural abundance, ease of enrichment, and the ability to minimise background noise, must be considered. Different isotopes exhibit varying half-lives and Q-values for $0\nu\beta\beta$ decay, which impacts their suitability for experiments. The main isotopes used and their corresponding experiments are analysed below.

Xenon-136

^{136}Xe is commonly used in experiments due to its high Q-value of 2.458 MeV, which stands out above many natural radioactivity backgrounds. Additionally, ^{136}Xe can be efficiently enriched and used in either liquid or gas form. Some recent experiments are summarised below.

KamLAND-Zen

The most well-known current experiment using Xenon is KamLAND-Zen, an extension of the KamLAND experiment located at the Kamioka Observatory in Japan, that has been collecting data since 2008. The detector consists of a large balloon filled with enriched xenon dissolved in a liquid scintillator, suspended within a much larger balloon filled with pure liquid scintillator. KamLAND-Zen has set some of the most stringent limits on the half-life of $0\nu\beta\beta$ decay, with a lower limit of 2.3×10^{26} years[38] based on results from KamLAND-Zen 800, the latest phase of the experiment.

EXO-200 and nEXO

EXO-200 was a completed experiment at the Waste Isolation Pilot Plant (WIPP) in New Mexico, running from 2011 to 2017. It utilised 200 kg of liquid xenon enriched to 80%

in ^{136}Xe and employed a time projection chamber (TPC) to detect and reconstruct $0\nu\beta\beta$ events. The TPC's capability to measure the energy and 3D positions of the decays effectively reduced background noise, setting a $0\nu\beta\beta$ half-life limit for ^{136}Xe at 1.8×10^{25} years[39]. Building on this success, nEXO is the next-generation experiment planned to expand to a 5-ton liquid xenon TPC, housed in a deep underground laboratory to further minimise cosmic ray interference. With advanced detection techniques, nEXO aims to improve sensitivity by about two orders of magnitude, targeting a $0\nu\beta\beta$ half-life sensitivity of around 10^{28} years[40].

Germanium-76

^{76}Ge is also used in various $0\nu\beta\beta$ decay experiments. Like Xenon, it has a favourable Q-value of 2.039 MeV and can be isotopically enriched. It is employed in semiconductor detectors that offer high energy resolution, which is crucial for distinguishing between signal and background. Although no current experiments use ^{76}Ge as their primary isotope, there are notable experiments to consider:

GERDA

The GERDA (GERmanium Detector Array) experiment, conducted at the Gran Sasso National Laboratory in Italy from 2011 to 2017, used high-purity germanium detectors enriched to about 86% in ^{76}Ge. A distinctive feature of GERDA was its use of liquid argon, which served both as a cooling medium and as a shield against external radiation. Additionally, the liquid argon acted as an active veto against background events: any particle interaction in the liquid argon that produced scintillation light would trigger a veto signal. GERDA set a lower limit on the ^{76}Ge $0\nu\beta\beta$ decay half-life at 1.8×10^{26} years[41], representing one of the most stringent constraints obtained.

LEGEND-1000

LEGEND-1000, presently being constructed at the Canfranc Underground Laboratory in Spain, will continue to use high-purity germanium detectors enriched in ^{76}Ge, but with several enhancements over its predecessors. Like GERDA, LEGEND-1000 will operate the detectors in a liquid argon environment, which serves as both a coolant and a background shield. Additionally, the collaboration will use pulse shape discrimination and segmentation in the germanium detectors to differentiate between signal events and background noise, further enhancing its sensitivity[42].

Apart from these, Molybdenum-100 is also a key candidate for $0\nu\beta\beta$ decay experiments due to its high Q-value of 3.034 MeV, which provides a significant advantage in reducing background noise. ^{100}Mo is used in various detector types, including scintillators and bolometers, with notable experiments involving NEMO-3 and its successor, SuperNEMO[43], which is currently under construction. Lastly, Tellurium-130 is appealing due to its high natural abundance, reducing the effort required for isotope enrichment, along with its Q-value of 2.527 MeV. Key ongoing experiments using ^{130}Te include CUORE[44] and SNO+[45].

Results

The table below summarises recent lower limits on the half-life $T^{0\nu}_{1/2}$ and corresponding upper bounds on the effective Majorana neutrino mass $m_{\beta\beta}$ for various neutrinoless double beta decay ($0\nu\beta\beta$) experiments. Experimentally, $m_{\beta\beta}$ and $T^{0\nu}_{1/2}$ are derived from the $0\nu\beta\beta$ decay rate:

$$\Gamma_{0\nu\beta\beta} = \frac{\ln 2}{T^{0\nu}_{1/2}} = G_{0\nu}|M_{0\nu}|^2|m_{\beta\beta}|^2 \tag{46}$$

Since $T^{0\nu}_{1/2}$ is inversely proportional to $m_{\beta\beta}$, measuring or constraining the half-life sets upper bounds on $m_{\beta\beta}$, thereby limiting the absolute neutrino mass scale.

Table 1 Experimental lower limits on $T^{0\nu}_{1/2}$ and corresponding upper bounds for $m_{\beta\beta}$, taking into account the NME theoretical uncertainties. The results for SNO+ are indicated with an asterisk ($*$) to denote predicted values, not yet measured experimentally.

Isotope	Experiment	$T^{0\nu}_{1/2}[y]$	$m_{\beta\beta}[eV]$
^{136}Xe	KamLAND-Zen	$> 2.3 \times 10^{26}$	$< 0.036 - 0.156$
^{136}Xe	EXO	$> 1.8 \times 10^{25}$	$< 0.15 - 0.52$
^{76}Ge	GERDA	$> 1.8 \times 10^{26}$	$< 0.09 - 0.29$
^{100}Mo	NEMO-3	$> 1.1 \times 10^{24}$	$< 0.31 - 0.96$
^{130}Te	CUORE	$> 2.2 \times 10^{25}$	$< 0.06 - 0.30$
^{130}Te	SNO+	$> 2.1 \times 10^{26*}$	$< 0.04 - 0.12^{*}$

The experimental results place $m_{\beta\beta}$ within a range of approximately 0.04–0.96 eV. These bounds impose constraints on the light neutrino mass through the relation $m_{\beta\beta} = \left|\sum_i U^2_{ei} m_i\right|$, where U_{ei} are elements of the PMNS matrix, and m_i are the light neutrino masses. If $0\nu\beta\beta$ is observed with a short half-life, implying a large $m_{\beta\beta}$, it suggests a lower right-handed neutrino mass M_R, favouring low-scale leptogenesis scenarios with $M_R \gtrsim 10^9$ GeV. Conversely, non-observation up to very long half-lives (beyond 10^{27} years) implies that lepton number violation at low energy is highly suppressed, supporting high-scale thermal leptogenesis where $M_R \gtrsim 10^{12}$ GeV.

These constraints highlight a fundamental tension between the neutrino mass scale and the viability of leptogenesis. The seesaw relation $m_\nu \approx -Y_D \nu M_M^{R\,-1} (Y_D \nu)^T$ implies that increasing the right-handed neutrino mass M_R while keeping m_ν within experimental bounds requires smaller Yukawa couplings. However, smaller Yukawa couplings reduce the CP asymmetry and can suppress the lepton asymmetry needed for baryogenesis. On the other hand, larger Yukawa couplings, which would enhance CP violation, also strengthen washout effects, potentially erasing the asymmetry.

Furthermore, constraints on $m_{\beta\beta}$ also restrict the allowed values of the Majorana phases in the PMNS matrix, which

influence the available CP violation for leptogenesis. If $m_{\beta\beta}$ is too small, it may indicate that the CP-violating phases are not optimally aligned for efficient leptogenesis, potentially reducing the generated baryon asymmetry.

Thus, the current experimental bounds on $0\nu\beta\beta$ play a key role in shaping viable leptogenesis models, linking the neutrino mass scale, CP violation, and lepton number violating processes.

Sources of Experimental Uncertainty

It is essential to evaluate the experimental uncertainties associated with the measurements of $m_{\beta\beta}$ and $T^{0\nu}_{1/2}$, which arise from multiple sources.

Statistical uncertainties arise from the limited number of observed events. Since $0\nu\beta\beta$ is extremely rare, experiments need long exposure times, and low statistics affect the precision of half-life estimates.

Systematic uncertainties stem from detector calibration, energy resolution, and detection efficiency. Poor energy resolution can blur the signal, increasing background interference. Calibration errors affect decay energy measurements, while uncertainties in efficiency—determined by material purity and event reconstruction—impact the reliability of detected events.

Background contamination further complicates measurements, as natural radioactivity, cosmogenic activation, and two-neutrino double beta decay can mimic or obscure a potential $0\nu\beta\beta$ signal. Experiments mitigate this with shielding, underground operation, and material selection, but residual noise remains a challenge.

Finally, theoretical uncertainties in nuclear matrix elements and phase space factors introduce significant variation in the extracted effective Majorana mass. While phase space factors are relatively well understood, nuclear matrix elements remain a major theoretical challenge, varying between different nuclear models. These variations introduce a factor of 2–3 uncertainty in the inferred $m\beta\beta$ limits, complicating the interpretation of experimental results in the context of neutrino mass constraints.

Other Experimental Evidence

Proton Decay

In the Standard Model, protons are considered stable due to the conservation of baryon number. However, many theories beyond the Standard Model predict that protons are not absolutely stable and could decay over extremely long timescales, with a half-life of at least 1.67×10^{34} years[46]. Proton decay is theorised to occur via the exchange of very heavy hypothetical gauge bosons, such as X or Y bosons, which mediate interactions violating baryon number conservation. The most common theoretical decay modes are $p \to e^+ + \pi^0$ and $p \to \mu^+ + \pi^0$, which violate baryon number by one unit.

Proton decay is relevant to leptogenesis because it directly violates baryon number conservation and involves leptons, suggesting a link between baryon and lepton number violations. The gauge bosons responsible for proton decay can mediate both types of violations, indicating an interconnection between these processes. Furthermore, many GUTs predict that the same interactions causing proton decay also produce the heavy right-handed neutrinos necessary for leptogenesis. Detecting proton decay would provide evidence for GUT-scale physics and support the likelihood of leptogenesis.

Lepton-Flavour Violating Decays

Lepton-flavour violating (LFV) decays occur when a lepton of one flavour decays into a lepton of a different flavour, accompanied by other particles, violating lepton flavour conservation. Key LFV decay channels include muon to electron and photon $\mu \to e\gamma$ and muon to electron conversion in nuclei $\mu \to eN$[47].

Many models that explain the generation of the lepton asymmetry needed for leptogenesis also predict LFV processes. If right-handed neutrinos or other particles involved in leptogenesis couple differently to different lepton flavours, they can induce LFV decays. Detecting LFV processes would thus provide indirect evidence for the new physics underlying leptogenesis.

Conclusion

Leptogenesis provides a compelling explanation for the matter-antimatter asymmetry in the universe, linking neutrino physics with cosmology. However, its viability hinges on the presence of substantial CP violation in the decay of heavy right-handed neutrinos, as well as the specific values of Yukawa couplings and the efficiency of sphaleron processes. The success of the mechanism is highly sensitive to these parameters, making it prone to fine-tuning. Additionally, the right-handed neutrinos required for leptogenesis are expected to have masses far beyond current experimental capabilities, and CP violation in the lepton sector has yet to be observed, meaning only indirect evidence is currently available. These factors limit direct experimental verification of the theory. Despite these challenges, leptogenesis remains a promising theoretical framework, and future experimental and observational advancements will be essential to addressing its limitations and assessing its validity.

Acknowledgements

I would like to express my sincere gratitude to Alex H. Adler from Stony Brook University for his invaluable guidance and support throughout the development of this research paper. His insightful feedback and expertise were crucial to the successful completion of this work.

References

1 W. Buchmüller, R. D. Peccei and T. Yanagida, *Annual Review of Nuclear and Particle Science*, 2005, **55**, 311–355.

2 S.-K. Collaboration and Y. Fukuda, *Physical Review Letters*, 1998, **81**, 1562–1567.

3 P. Minkowski, *Physics Letters B*, 1977, **67**, 421–428.

4 T. Yanagida, *Progress of Theoretical Physics*, 1980, **64**, 1103.

5 W. Pauli, *Physics Today*, 1930, **31**, 27.

6 E. Fermi, *Nuovo Cimento*, 1934, **11**, 1–19.

7 C. L. C. Jr., F. Reines, F. B. Harrison, H. W. Kruse and A. D. McGuire, *Science*, 1956, **124**, 103–104.

8 P. D. Group, *Progress of Theoretical and Experimental Physics*, 2023, **2023**, 083C01.

9 P. W. Higgs, *Physical Review Letters*, 1964, **13**, 508–509.

10 I. Esteban, M. C. Gonzalez-Garcia, M. Maltoni, T. Schwetz and A. Zhou, *Journal of High Energy Physics*, 2020, **09**, 178.

11 P. Collaboration, *Astronomy Astrophysics*, 2020, **641**, A6.

12 M. Drewes and J. Maalampi, *Physical Review D*, 2019, **100**, 075029.

13 P. A. M. Dirac, *Proceedings of the Royal Society of London. Series A*, 1928, **117**, 610–624.

14 C. D. Anderson, *Physical Review*, 1933, **43**, 491–494.

15 G. Lemaître, *Annales de la Société Scientifique de Bruxelles*, 1927, **A 47**, 49–59.

16 E. Hubble, *Proceedings of the National Academy of Sciences*, 1929, **15**, 168–173.

17 G. Gamow, *Physical Review*, 1946, **70**, 572–573.

18 B. D. Fields, P. Molaro and S. Sarkar, *Chinese Physics C*, 2014, **38**, 339–344.

19 R. H. Cyburt, B. D. Fields, K. A. Olive and T.-H. Yeh, *Reviews of Modern Physics*, 2016, **88**, 015004.

20 A. D. Sakharov, *Pisma Zhurnal Ekspperimentalnoi i Teoreticheskoi Fiziki*, 1967, **5**, 32–35.

21 R. Jackiw and C. Rebbi, *Physical Review Letters*, 1976, **37**, 172–175.

22 M. Pospelov and A. Ritz, *Annals of Physics*, 2005, **318**, 119–169.

23 C. Abel, N. J. Ayres, G. Ban, G. Bison, K. Bodek, M. Burghoff, E. Chanel, P. Chiu, C. B. Daigle and e. a. M. Daum, *Physical Review Letters*, 2020, **124**, 081803.

24 M. Kobayashi and T. Maskawa, *Progress of Theoretical Physics*, 1973, **49**, 652–657.

25 J. H. Christenson, J. W. Cronin, V. L. Fitch and R. Turlay, *Physical Review Letters*, 1964, **13**, 138–140.

26 B. A. BaBar Collaboration, *Physical Review Letters*, 2001, **87**, 091801.

27 L. Collaboration, *Journal of High Energy Physics*, 2014, **2014**, 041.

28 J. M. Cline, *Baryogenesis*, 2006.

29 V. A. Kuzmin, V. A. Rubakov and M. E. Shaposhnikov, *Physics Letters B*, 1985, **155**, 36–42.

30 M. Fukugita and T. Yanagida, *Physics Letters B*, 1986, **174**, 45–47.

31 S. Banerjee, P. S. B. Dev, A. Ibarra, T. Mandal and M. Mitra, *Physical Review D*, 2015, **92**, 075002.

32 Y. Zhang, H. An, X. Ji and R. N. Mohapatra, *Nuclear Physics B*, 2008, **802**, 247–279.

33 J. Chakrabortty, *Physics Letters B*, 2010, **690**, 382–385.

34 L. Covi, E. Roulet and F. Vissani, *Physics Letters B*, 1996, **384**, 169–174.

35 N. S. Manton, *Philosophical Transactions of the Royal Society A: Mathematical, Physical and Engineering Sciences*, 2019, **377**, 20180327.

36 U. Sarkar, *Baryogenesis through lepton number violation*, 1998.

37 G. D. Moore, *Physical Review D*, 1999, **59**, 014503.

38 K.-Z. Collaboration, *Physical Review Letters*, 2023, **130**, 051801.

39 E.-. Collaboration, *Physical Review Letters*, 2018, **120**, 072701.

40 nEXO Collaboration, *Journal of Physics G: Nuclear and Particle Physics*, 2022, **49**, 015104.

41 G. Collaboration, *Physical Review Letters*, 2020, **125**, 252502.

42 L. Collaboration, AIP Conference Proceedings, 2017, p. 020027.

43 T. L. Noblet, NEMO-3 and S. Collaborations, Journal of Physics: Conference Series, 2020, p. 012029.

44 C. Collaboration, Proceedings of Science: ICHEP2022, 2022.

45 J. Paton, *Neutrinoless double beta decay in the SNO+ experiment*, 2019.

46 B. Bajc, J. Hisano, T. Kuwahara and Y. Omura, *Nuclear Physics B*, 2016, **910**, 166–189.

47 L. Galli, Flavor Physics and CP Violation Conference (Victoria BC, 2019), 2019.